Geomechanics and Engineering, *Vol. 41, No. 6 (2025) 611-623*
https://doi.org/10.12989/gae.2025.41.6.611

Reliability analysis of tunnel-type anchorage in suspension bridge based on the second-order response surface method

Guojun Yang*[1], Shutao Zhang[1a], Yongfeng Du[1b] and Guangwu Tang[2c]

[1]*Western Engineering Research Center of Disaster Mitigation in Civil Engineering of the Ministry of Education, Lanzhou University of Technology, Lanzhou 730050, China*
[2]*State Key Laboratory of Bridge Engineering Structural Dynamic,China Merchants Chongqing Communications Technology Research & Design Institute Co., Ltd. Chongqing,400067,China*

(*Received October 10, 2024, Revised March 29, 2025, Accepted May 8, 2025*)

Abstract. In recent years, tunnel-type anchorage (TTA) has been increasingly applied in long-span suspension bridges. However, research on its reliability analysis under seismic effects remains insufficient. This study takes the Puli Bridge in Yunnan Province, China, as an example to investigate the dynamic response and reliability of the TTA of a suspension bridge under seismic action. The dynamic response of ten measurement points on the front and rear anchor faces of TTA under seismic acceleration was calculated and analyzed using finite difference method software. Combining the secondary sequence response surface method, the reliability indices of each measurement point on the anchor surface before and after TTA were calculated and analyzed, and the limit state equation of TTA dynamic response was established. The results indicate that the elastic modulus and cohesion of the TTA surrounding rock have a significant influence on the dynamic response of the TTA. The dynamic response of TTA decreases with increasing elastic modulus and increases with increasing cohesion. As shown in its displacement response. Due to the design characteristics of TTA, the reliability value of the front anchor surface is significantly lower than that of the rear anchor surface. Under different peak ground accelerations (PGA), the reliability of different cross-sections of TTA varies and decreases with increasing PGA, indicating that the reliability of TTA is highly sensitive to changes in PGA. Research on the dynamic response and reliability of the front and rear anchor surfaces of TTA structures can provide reference and assistance for the seismic retrofitting and optimization design of TTA structures.

Keywords: bridge and tunnel engineering; dynamic response; ground motion acceleration; reliability analysis; tunnel-type anchorage

1. Introduction

As one of the main components of suspension bridges, TTA primarily bear the immense tensile loads transmitted by the main cables, transferring these forces to the surrounding rock mass near the TTA (Wu.*et al*. 2023, Han *et al*. 2023a, b, Shen *et al* 2022). Due to the complex load-bearing mechanism of TTA, their effective application requires favorable geotechnical conditions around the anchorage. Therefore, studying their reliability under external excitations, such as earthquakes, is crucial for ensuring the overall safety performance of suspension bridges (Ali *et al*. 2024, Yasir *et al*. 2024, Niccolò *et al*. 2024, Anno *et al*. 2024, Suzana *et al*. 2024). Traditional reliability assessment methods for geotechnical and underground engineering often rely on complex mathematical calculations and extensive field test data, which are not only time-consuming and labor-intensive but also somewhat lacking in accuracy. The second-order response surface method, based on experimental design and statistical analysis (Sara *et al*. 2016, Namitha *et al*. 2024, Anjneya *et al*. 2021, Van *et al*. 2021, Usman *et al*. 2021), establishes an approximate relationship model between dependent and independent variables. This method is widely used in engineering optimization and quality improvement fields. This study attempts to apply the second-order sequential response surface method to the reliability model calculation of suspension bridge TTA, aiming to improve the predictive accuracy and evaluation efficiency of the model. In geotechnical engineering, traditional methods used to analyze the stability of slopes and rock masses(Rao *et al*. 2021), such as the first-order second-moment method, the first-order second-moment method's central point method (JC method), and the Monte Carlo method (Krüger *et al*. 2023, Kranz *et al*. 2023, Dittmann *et al*. 2022, Taesuk *et al*. 2025, Bossoto *et al*. 2023), inevitably involve cumbersome calculations and extensive data statistics, with accuracy falling short of scientific research requirements. Although the first-order second-moment method is simple and practical, its convergence and accuracy need improvement for complex geotechnical engineering (Kumar *et al*. 2024, Verma *et al*.

*Corresponding author, Professor
E-mail: yanggj403@163.com
[a]M.Eng. Student
E-mail: 1353671454@qq.com
[b]Professor
E-mail: dooyf@sohu.com
[c]Professor
E-mail: tangguangwu@cmhk.com

ISSN: 2005-307X (Print), 2092-6219 (Online)

2024, Paprocki *et al*. 2024, Sachin *et al*. 2024, Joseph *et al*. 2024). Particularly when considering external dynamic loads such as earthquakes, the application of this method no longer meets the demands of actual scientific research and engineering applications. Wang *et al*. (2024) used the Monte Carlo method to calculate the reliability index of typical service time points of cracking linings. The study concluded that the crack stress intensity factor is positively correlated with the crack opening depth. As the crack opening depth increases, the structural reliability index decreases. However, this method requires a large amount of data for sampling calculations, making the calculation process cumbersome. Li *et al*. (2023) utilized interval theory to represent uncertain parameters in interval form. Then, considering the coexistence of multiple failure modes in rock tunnel engineering, the concept of structural system reliability was introduced, and a calculation method based on interval non-probability for the reliability index of rock tunnel structural system and its stability evaluation were established (Fernandez *et al*. 2022, Özge *et al*. 2024, Taslimi *et al*. 2024). Based on this, the rationality of this method was verified through engineering examples. This method can effectively avoid the need for a sufficient number of statistical sample information of random parameters to construct probability density distribution function in traditional reliability calculation methods. However, the calculation process is too complex. As one of the most important load-bearing components of a suspension bridge, the selection of a suitable reliability calculation and analysis method for suspension bridge TTA becomes necessary (Lim *et al.* 2021). Wang *et al*. (2020) analyzed the force transmission throughout the entire construction process from TTA construction to the completion of the bridge. A simplified mechanical model for TTA was established, the distribution of compressive stress generated by the load acting on the anchor-rock interface along the axial direction of the anchorage plug was analyzed, and a calculation formula for the ultimate bearing capacity of TTA was provided. This also laid a solid foundation for the calculation of the reliability of suspension bridge TTA under static loads. Liu *et al*. (2020) extensively studied the reliability of TTA using finite element software to evaluate the safety factor of TTA. They also established a prediction model for the safety factor of TTA using artificial neural network methods. Since then, the reliability research of TTA has gradually attracted attention from experts and scholars. Yu (2021) used neural networks and first-order reliability analysis methods to study the reliability of this TTA's safe operation. The research mainly focused on the reliability of TTA under static loads and did not consider the reliability under seismic excitations.

Since earthquakes can cause damage to large underground infrastructure such as tunnels and TTA structures, particularly in the southwestern region of China located along the Pacific Ring of Fire where earthquakes occur frequently, they can have a certain impact on the reliability of TTA. Therefore, it is crucial to study the reliability of suspension bridge TTA under seismic loads. This study combines finite difference software calculations with the second-order response surface analysis method of mathematical probability statistics. Taking the Puli Bridge in Yunnan Province as an example, this study analyzes the reliability of the TTA system, providing reference for the pre-reinforcement of TTA systems in suspension bridges under seismic loads. The aim is to effectively reduce the risk of damage to the overall structure of suspension bridges during earthquakes.

2. Finite difference software simulation

2.1 Boundary conditions

This study analyzes the key reliability issues of the Puli Bridge and its TTA in Yunnan Province, China. The Puli Bridge spans the Puli River at 11+233.807 to 12+237.000 kilometers on the Puxuan Expressway and is an important control project in the local area. The background bridge is a single-span simply supported steel box girder suspension bridge with a main span of 628 meters and a side span of 166 meters. The tower structure adopts a column-type portal frame design, constructed on a pile foundation. Fig. 1 shows the specific location of the Puli Bridge. The Puli end employs a TTA system, while the Xuanwei end utilizes a gravity anchor system.

The geological conditions of Puli End include limestone from the Maoping Formation (C3mp) of the Upper Permian, characterized by intense karstification and extensive shallow fractures, resulting in severe rock fragmentation. Below 30 meters, the rock mass is relatively intact, with karst phenomena observed only in the fractures. The TTA anchor plugs are mainly located in Class III and IV rock bodies, with some located in Class V fissured rock bodies that have been significantly affected by karstification. The simulation analysis in this paper mainly uses finite difference software. A certain degree of normalization processing has been performed. Based on actual engineering data, the TTA dimensions of the model were determined. The dimensions of the slope model are 150 m × 150 m × 150 m, as shown in Fig. 2 of the finite difference software model. The model contains 20,671 nodes and 109,098 elements. The applied boundary conditions include triaxial constraints at the bottom, normal constraints around the perimeter, and free conditions at the top.

The TTA has an inverted wedge shape, with its anchorage face resembling a castle gate, and specific dimensions: the front anchorage chamber is 30 m long, the entire anchorage plug is 35 m long, the rear anchorage chamber is 3 m long, and the anchorage plug body has an inclination angle of 42°.The front anchor face is 9.5 meters wide, and the rear anchor face is 13 meters wide, as shown in Fig. 2. In dynamic analysis, selecting appropriate boundary conditions around the model is critical to ensuring the accuracy of the computational results. This is because wave reflection may occur at the model boundaries, thereby affecting the results of the dynamic analysis. Therefore, during dynamic calculations, boundary conditions differ from static conditions. Initially, static boundary conditions are removed, and free-field boundary conditions are applied around the perimeter, with static boundaries maintained at the bottom. The selection of

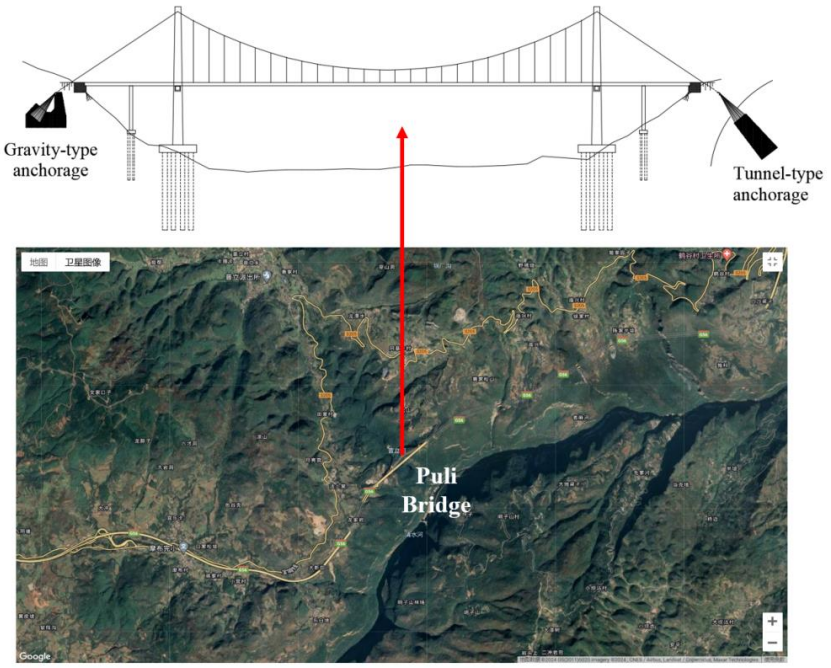

Fig. 1 Location and structure diagram of Puli Bridge in Yunnan Province (2025)

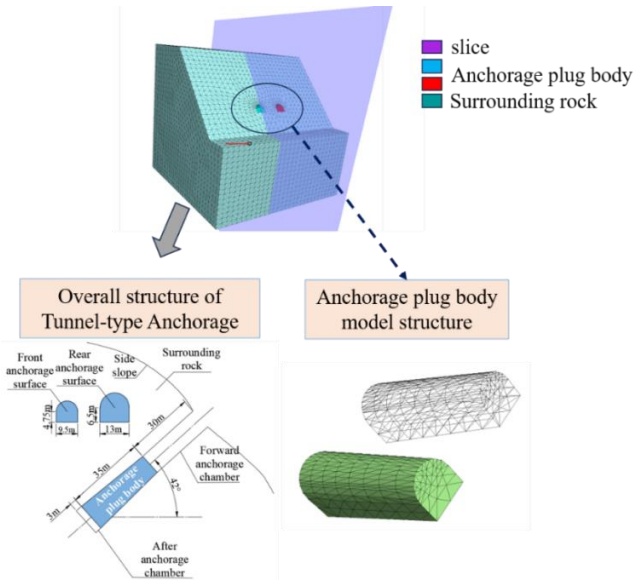

Fig. 2 TTA structure and model diagram of suspension bridge

boundary conditions around the model perimeter is critical in dynamic analysis due to the potential impact of wave reflections on the results.

2.2 Material characteristics

When using finite difference method software to simulate the construction process of an actual engineering project, the surrounding rock is idealized to simplify calculations and improve computational efficiency. So certain assumptions were made: the rock mass was modeled using the Mohr-Coulomb constitutive model, and the anchorage body was modeled using a linear elastic constitutive model. It was assumed that the surrounding rock is a homogeneous rock mass, neglecting the anisotropy of the rock. The rheological properties of the rock mass and anchor plugs were idealized. Parameters used in the numerical simulation were determined based on field survey data, standards, and inverse analysis of displacement. Due to the need to modify some experimental parameters for reliability calculations using the second-order response surface method (Cao *et al* 2015), the parameters of the rock mass with smaller coefficients of variation in the model were standardized to primarily reflect the properties of the main rock mass. The computational parameters of the resulting numerical model are shown in Table 1.

Table 1 Numerical model parameters

Materials	Severe ($N \cdot m^{-3}$)	Bulk modulus (Pa)	Shear modulus (Pa)	Cohesion (Pa)	Angle of internal friction (°)	Tensile strength (Pa)
Surrounding rock	2803	2×10^{10}	1.45×10^{10}	0.8×10^{6}	37.5	0.525×10^{6}
Anchorage plug body	2600	1.47×10^{10}	1.29×10^{10}	-	-	-

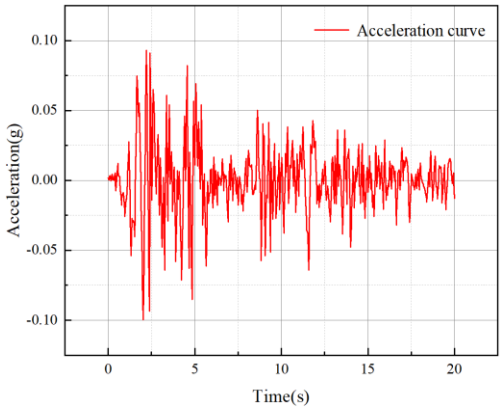

Fig. 3 El-Centro wave after artificial modification

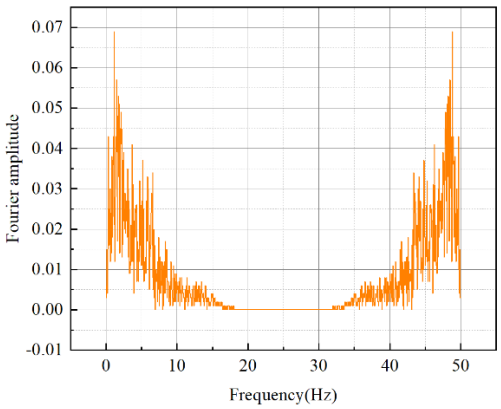

Fig. 4 Fourier spectrum of El-Centro wave after artificial modification

The construction steps for simulating the actual engineering conditions during numerical analysis are as follows:

(1) Utilize modeling and meshing software to draw the slope and anchorage body, and refine the mesh.

(2) Simulate the initial in-situ stress equilibrium before tunnel-type excavation in the actual project, and assign values to the model.

(3) Simulate the excavation steps of the actual anchorage hole in the model and cast the anchorage body.

(4) In the software, simulate the cable force of the suspension bridge, with a value of p = 101202 kN, applied to the rear anchorage face of the anchorage body.

(5) Input seismic acceleration to simulate the response of the entire slope under seismic action.

2.3 Seismic acceleration retrofit input

To conduct reliability analysis, it is necessary to simulate the dynamic response of the suspension bridge TTA under seismic excitation. Therefore, the required seismic data was downloaded from the Pacific Earthquake Engineering Research Center (PEER), and the first 20 seconds of the El-Centro seismic wave data record were selected for this study. Since the existing seismic acceleration data cannot be directly imported into the finite difference software (Małgorzata *et al*. 2024), the data needs to be corrected and filtered. The peak acceleration of the data at the bottom of the model was adjusted to 0.1 g. Fig. 3 shows the adjusted El-Centro wave. Using Eqs. (1) and (2), the seismic acceleration was converted into stress and input from the bottom of the constructed slope model, as shown in Fig. 5. For incident waves with an incident angle greater than 30°, the static boundary can fully absorb them. However, when the incident angle is smaller, the static boundary has a certain absorption capacity but is not complete. If dynamic loads are to be applied at the static

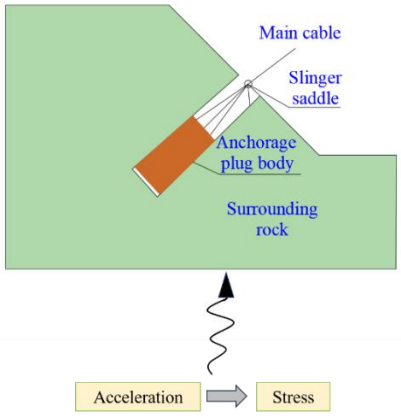

Fig. 5 Input direction of ground motion acceleration

boundary, only stress time histories can be input. Acceleration and velocity time histories can be converted into stress time histories using the conversion formulas (1) and (2). Fig. 4 shows the Fourier spectrum of the manually modified El-Centro wave. As can be seen from Fig. 4, the main effect of the El-Centro wave is within 20 Hz. Therefore, during filtering correction, the seismic acceleration before 20Hz is mainly used.

$$Cs=\sqrt{\frac{G}{\rho}} \tag{1}$$

$$\sigma_s = -2(\rho C_s) V_s \tag{2}$$

where *Cs* is the wave velocity, *G* is the shear modulus, ρ is the density, σ_s is the stress in the shear direction, and Vs is the velocity.

Fig. 5 illustrates the simulation of the overall seismic acceleration input. Since existing finite difference analysis

Table 2 Bucher designed the experimental parameters

Experimental condition	Experimental point	f-value	Design formula
1	C, E	2	$X_i = \mu_i \pm f\sigma_i$
2	$C, E + 2\sigma$	2	
3	$C, E - 2\sigma$	2	
4	$C + 2\sigma, E$	2	
5	$C - 2\sigma, E$	2	

software cannot directly apply seismic acceleration on static boundaries, it is necessary to use established formulas to convert filtered and corrected seismic acceleration data. In this process, SeismoSignal software and Eqs. (1) and (2) are used for the necessary conversions.

3. Seismic dynamic response analysis

Using finite difference software simulation and a second-order response surface method with cross-term elimination, Bucher experiments were designed to classify parameters with high coefficient of variation into five operating conditions for calculation. Particular attention was paid to the rock cohesion (C) and elastic modulus (E) listed in Table 2. Since the statistical coefficient of variation for these two parameters exceeded 0.2, it indicates that they have a significant influence on the deformation of the surrounding rock around the anchor block. In dynamic analysis, changes in these two parameters of the surrounding rock around the anchor also significantly affect the dynamic response of the anchor under seismic acceleration.

Therefore, the aforementioned parameters were selected for the calculation of working conditions, with the specific experimental design detailed in Table 2. Through this experimental design and calculation process, it is possible to more accurately assess the deformation of the rock mass surrounding the anchor blocks under different working conditions, providing reliable data support for the dynamic response of TTA during seismic motion.

$X_i = \mu_i \pm f\sigma_i$ where $\mu_i$is the mean value, f is typically set to 2 based on empirical formulas in geotechnical engineering, and σ_i is the standard deviation.

In engineering practice, the anchorage blocks of suspension bridges are generally cast using reinforced concrete, which has an extremely low probability of brittle failure. Therefore, most experts and scholars primarily study the mechanical properties and reliability of the anchorage blocks by analyzing the changes and reactions of the surrounding rock mass, in order to evaluate the safety of the TTA and the entire bridge. Fig. 6 shows the monitoring points arranged on the rock contact surface to record the dynamic response of the TTA. Five monitoring points are set on the front anchor face, and five monitoring points are also set on the rear anchor face. This layout aims to better monitor the impact of seismic excitation on the entire anchor plug. Since the anchor plug is regarded as an ideal elastic whole in the modeling process, the monitoring points

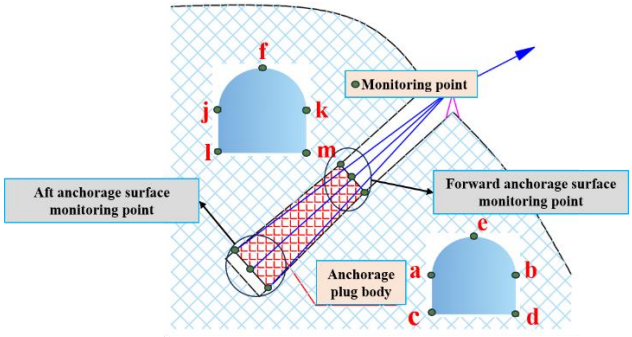

Fig. 6 Schematic diagram of monitoring site layout

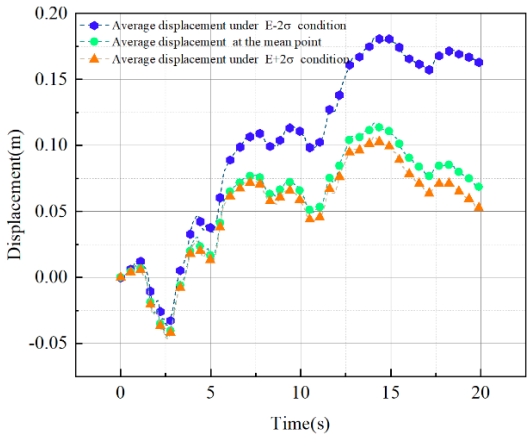

(a) Comparison of mean displacement under different elastic modulus

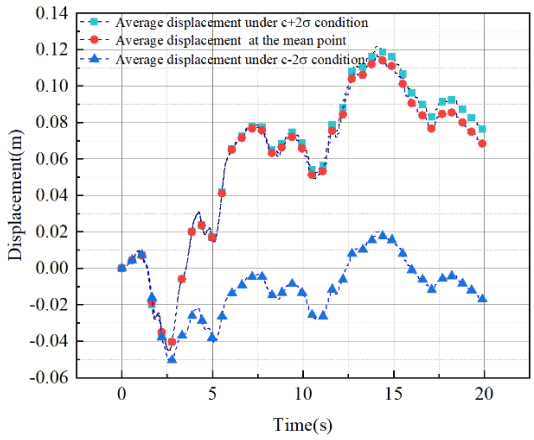

(b) Comparison of mean displacement under different cohesion forces

Fig. 7 Comparison of average displacement of monitoring points under different working conditions

should be set on the anchor-rock contact surface rather than on the anchor plug surface.

By adjusting parameters based on statistical data (specific calculation methods are detailed below), the parameters for the initial experimental points (average points) can be determined. Displacement velocity data of the dynamic response of the front and rear anchor surfaces under seismic acceleration within 20 seconds were calculated. Figs. 7 and 8 show that the elastic modulus and cohesion of the surrounding rock mass around the TTA significantly influence its mechanical response

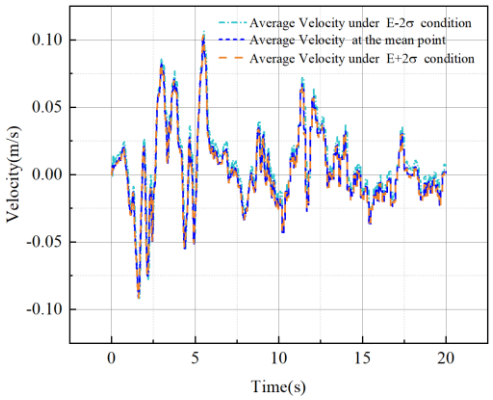

(a) Comparison of mean velocity under different elastic modulus

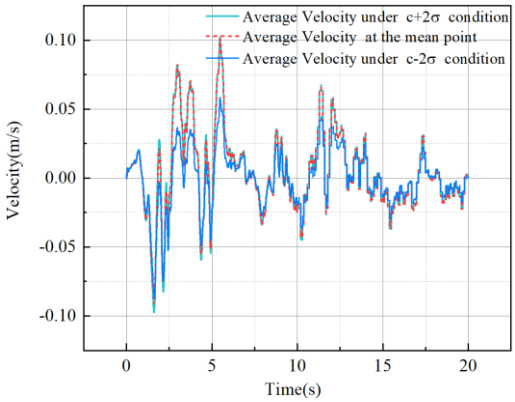

(b) Comparison of mean velocity under different cohesion forces

Fig. 8 Comparison of average velocity of monitoring points under different working conditions

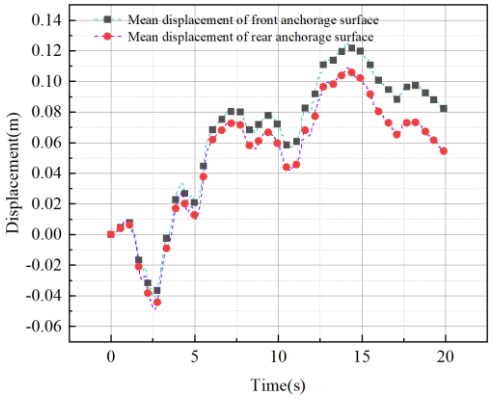

(a) Comparison of mean displacement of front and rear anchorage surfaces

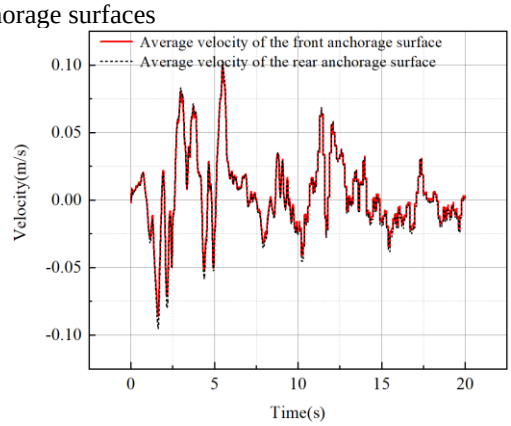

(b) Comparison of average velocity between front and rear anchorage surfaces

Fig. 9 Comparison of average displacement velocities of monitoring points on the front and rear anchorage surfaces

under seismic excitation. According to Fig. 7(a), the smaller the elastic modulus of the TTA, the more sensitive its response to seismic excitation. Under E-2σ conditions, the maximum average displacement of the front and rear anchor faces was 55.6% higher than the average point displacement, as shown in Fig. 8(a).This indicates that the displacement results in Fig. 7(a) are accurate. This sensitivity stems from the elastic modulus, which reflects the deformation capacity of the surrounding rock material under stress. Materials with higher elastic moduli typically exhibit greater stiffness and hardness, resulting in weaker dynamic responses under seismic excitation.

As shown in Fig. 7(b), higher cohesion causes the anchor plug to exhibit a more pronounced displacement response to seismic excitation. Under c-2σ conditions, the maximum average displacement is 4.57 times lower than the average point displacement value, as shown in Fig. 8(b). This chart indicates that under these conditions, the average velocity of the front and rear anchor faces is 72.4% higher than the velocity value under c-2σ conditions, which suggests that the increase in cohesion strength enhances the dynamic response of the anchor plug body and the surrounding rock mass under seismic excitation. This phenomenon is caused by the fact that highly cohesive materials are typically denser, resulting in slower seismic wave propagation speeds. When seismic waves pass through these materials, they encounter greater resistance, releasing more energy and triggering stronger seismic responses. In addition, high cohesion also causes seismic waves to scatter and reflect, making their propagation paths within the material more complex. When seismic waves pass through the TTA, they interact with the TTA structure, thereby amplifying the magnitude and intensity of the earthquake. The enhanced cohesion alters the velocity of seismic waves, particularly at stratigraphic interfaces or geological transitions, causing refraction and reflection of seismic waves. This further enhances the interaction between seismic waves and geological structures, exacerbating the impact of the earthquake.

As shown in Fig. 9(a), the average displacement values of the anchor faces before and after TTA were compared. The data indicate that the average displacement value of the front anchor face is 25% higher than that of the rear anchor face. In Fig. 9(b), the average velocity response at five measurement points on the rear anchor face is 50.8% lower than that on the front anchor face. As the slope height decreases, the displacement fluctuations of the rock mass around the anchor plug gradually decrease, indicating the presence of the “whip effect” (Hu *et al.* 2024). As the slope height increases, this effect tends to strengthen. Additionally, compared to the rear anchor face, the dynamic response of the front anchor face is more pronounced, indicating the cantilever face effect (Huang *et al*. 2016).

Table 3 Statistical table of parameters of TTA

Bridge name	Angle of inclination β (°)	Angle of internal friction φ (°)	Elastic modulus of s urrounding rock E (GPa)	Poisson's ratio μ	Cohesive force c (kPa)
Lijiang Jinsha River Bridge	35	34.6	3.2	0.3	400
Lvzhijiang Bridge	35	33	4.6	0.28	900
Yichang Wujiagang Bridge	40	32	1.1	0.33	800
Hubei Sidu River Bridge	35	35.2	4	0.26	1100
Puli Bridge	42	37.5	2.5	0.23	1000
Aizhai Bridge	38	37	5	0.26	800

Table 4 Statistical characteristics of TTA surrounding rock parameter variables

Surrounding rock parameter	Angle of inclination β (°)	Angle of internal friction φ (°)	Elastic modulus of surrounding rock E (GPa)	Poisson's ratio μ	Cohesive force c (kPa)
Mean value	38	35	3.4	0.28	833
Standard deviation	2.78	1.97	1.32	0.03	221.11
Coefficient of variation	0.07	0.06	0.39	0.11	0.27

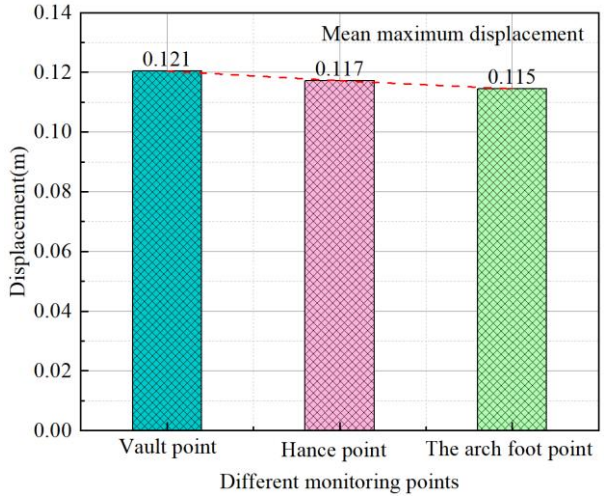

Fig. 10 Maximum average displacement at different monitoring points

The overall integrity of the TTA front anchor chamber is poor, often leading to rock mass failure, typically starting from the front anchor face of the TTA front anchor chamber.

In Fig. 6, monitoring points e and f are defined as crown measurement points, while points j, k, a, and b are defined as arch waist measurement points, and points c, d, l, and m are defined as arch toe measurement points. According to the finite difference simulation results in Fig. 10, under seismic excitation, the displacement values at the arch crown are the largest, followed by those at the arch waist points, and finally those at the arch toe points. The maximum average displacement at the arch toe points is 3.4% higher than that at the arch waist points and 5.2% higher than that at the arch crown points. This is due to the reflection and refraction of seismic waves when encountering different media.

The arch measurement points of the TTA are proximate to the ground and receive a greater number of reflected waves, thereby enhancing its dynamic response. Additionally, under seismic excitation, the TTA structure is affected by inertial forces. Due to the TTA arch's low mass, the forces of inertia it experiences are comparatively negligible. However, its displacement relative to the ground is substantial, resulting in a more pronounced dynamic response.

4. Tunnel-type anchorage reliability analysis

4.1 Second-order response surface method

The second-order response surface method is a well-established statistical modeling technique in the field of mathematical statistics. It is primarily used to determine the optimal combination of multiple input variables that influence a specific output variable. The specific application steps are as follows: first, a set of central points and boundary points must be identified. Experiments are then conducted at these points to collect data on the response variable. Finally, the data is fitted using a quadratic polynomial model to establish a regression model between the response variable and the input variables. This mathematical statistical method can predict the optimal combination of input variables to achieve optimization. The method uses the least squares method to fit the polynomial regression model, followed by statistical methods for parameter estimation and model comparison. Based on the established model, the optimal values of the response variable and the response surface can be calculated, thereby determining the optimal combination of input variables. As shown in Table 3, statistical information on parameters such

as the elastic modulus and internal friction angle of six types of TTA rock bodies in China is provided.

Table 4 shows the statistical characteristics of the variable parameters of TTA rock. The mean values, standard deviations, and coefficients of variation were calculated for different rock body parameters, and parameters with high coefficients of variation, such as elastic modulus and cohesion, were identified and set as variables. Formula (3) is the expression for the coefficient of variation (CV) of the surrounding rock parameters in the tunnel anchorage, which quantifies the relative dispersion of the dataset for these parameters.

$$CV = \frac{\sigma}{\mu} \tag{3}$$

where σ is the standard deviation of the dataset, and μ is the mean of the dataset.

This method is specifically designed for reliability calculations in TTA. Since parameters such as the elastic modulus and internal friction angle follow a normal distribution, their average values are used as the central points for calculations. According to the formula $\mu_x \pm f\sigma_x$, parameters with a coefficient of variation exceeding 0.2 will undergo dynamic calculations under the five different operating conditions mentioned in Table 2.

4.2 Second-order response surface method function and limit state equation

In the context of contemporary research endeavors, the formulation of limit state equations for TTA structures predominantly hinges on a modeling framework that incorporates resistance and load effects. Existing reliability assessment methodologies are predicated on the assumption that limit state equations possess precise analytical expressions. However, for TTA structural systems, the inherent complexity of these systems can result in highly nonlinear relationships between the inputs and outputs of basic random variables. In such cases, the existence of clear analytical expressions may be dubious. Consequently, when attempting to calculate the reliability of these complex structures, traditional reliability analysis models cannot be determined in advance. This is not conducive to our reliability research on large structures, such as the TTA. The second-order response surface method is an innovative tool in reliability analysis that provides an effective way to model and calculate the reliability of complex structural systems. As illustrated in Fig.11, the calculation of the TTA reliability can be performed in a stepwise manner. Initially, the selection of the mean value points is conducted, followed by the determination of the functional coefficient value through the Bucher test design. This process enables the identification of the value of the coefficient matrix. Subsequently, the MATLAB program is utilized to obtain the desired result.The initial stage of the process involves the calculation of the reliability index for each specific monitoring point. This study successfully addressed the nonlinearity issues of the TTA that are difficult to handle using traditional methods by constructing an approximate response surface model. This opens up new avenues for the reliability assessment of complex structures. The response

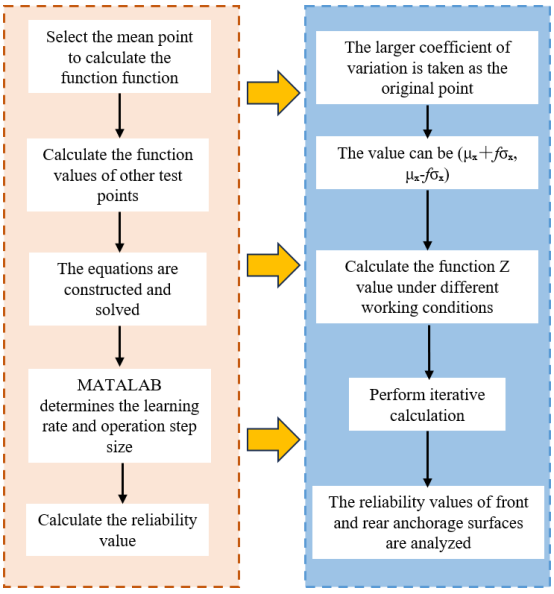

Fig. 11 Flow chart of reliability calculation

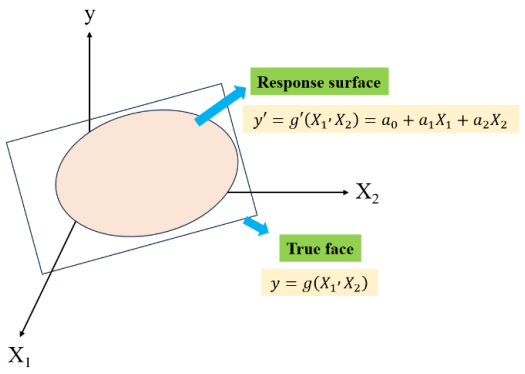

Fig. 12 Geometric representation of linear response surfaces of double random variables

surface function must satisfy two conditions. First, it should be concise and clear, accurately reflecting the true functionality. Second, the number of uncertainty coefficients in the design should be minimized. Based on these requirements, the first-order response surface function can be expressed as follows

$$y' = g'(X_1, X_2 \ldots X_n) = a_0 + \sum_{i=1}^{n} a_i x_i \tag{4}$$

The form of the Second-Order Response Surface function is

$$y' = g'(X_1, X_2 \ldots X_n) = a_0 + \sum_{i=1}^{n} a_i x_i + \sum_{i=1}^{n} b_i x_i \tag{5}$$

where a_0, a_i, b_i are the undetermined and corrected coefficients of the expression respectively.

Based on the analysis of the variability of rock parameters around the TTA, this study selected the elastic modulus and cohesion of the tunnel surrounding rock as variables. Fig. 12 shows the geometric representation of the linear response surface of the two random variables (elastic modulus and cohesion).

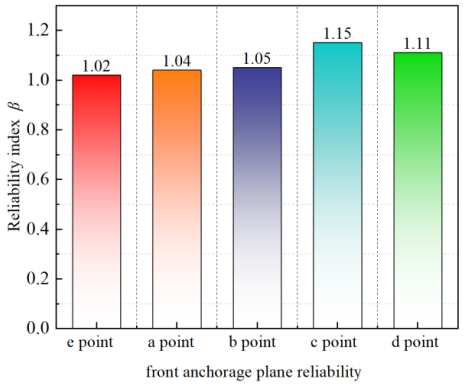

(a) front anchorage plane reliability

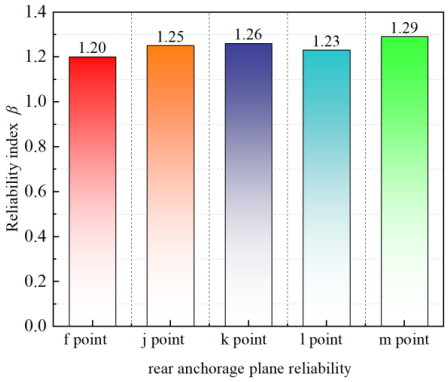

(b) rear anchorage plane reliability

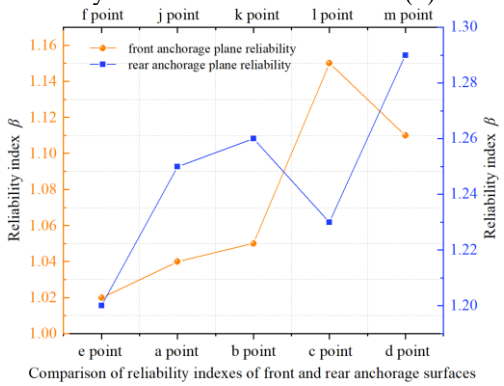

(c) Comparison of reliability indexes of front and rear anchorage surfaces

Fig. 13 Reliability value of anchorage surface at front and rear of TTA

Under non-rock foundation conditions, TTA will inevitably experience horizontal displacement and settlement when subjected to cable tension and seismic excitation. Since horizontal displacement poses a significant threat to bridge safety, this discussion focuses primarily on horizontal displacement. In the operational state of the bridge after construction, these displacements of TTA will significantly influence the load-carrying characteristics of the entire bridge. Therefore, adequate consideration must be given during design. The discussion here pertains to the X-direction, which is also the direction of cable forces acting on TTA in suspension bridges. Based on this, the limit state equations are provided as follows

$$G(x) = S_{\max} - S_j = a_0 + \sum_{i=1}^{2} a_i x_i + \sum_{i=1}^{2} b_i x_i \tag{6}$$

where a_0, a_i, b_i is the undetermined constant, it can be solved by interpolation method. S_{max} is the maximum displacement and deformation value, and S_j is the simulation result of finite difference software.

$$min\,\beta^2 = \sum_{i}^{n} [(x_i - u)/\sigma]^2 \tag{7}$$

Where β is the reliable index, x_i is the result after iterative calculation, μ is the mean value, and σ is the standard deviation.

Using Eqs. (6) and (7) and the data in Table 4, a calculation program integrating a high-precision gradient optimization algorithm was developed using commercial mathematical software. This program can calculate the reliability index β of each monitoring point on the front and rear anchor surfaces, as shown in Fig. 13. From Fig. 13, it is evident that under seismic excitation, the reliability of the front anchorage surface in the tunnel is notably lower than that of the rear anchorage surface. This discrepancy arises because the front anchorage surface is located within the front anchorage chamber without soil or rock mass in front, resulting in an exposed face effect. Consequently, the response of the front anchorage surface is more severe under seismic excitation, leading to reduced reliability. In Figs. 13(a)-13(c) it is observed that the reliability is higher at the arch foot of the TTA. This is attributed to significant influences from the self-weight of the anchorage block on the surrounding rock below, resulting in substantial bearing of pressure and shear forces by the surrounding rock. Particularly in the bottom corner areas on either side of the anchorage block, stress concentration phenomena are notably pronounced, thereby attenuating the dynamic response in that region.

5. The impact of different PGAs on the reliability of suspension bridge tunnel-type anchorage

By manually adjusting the PGA (peak ground acceleration) of the EL-Centro wave, the influence of different PGAs on the reliability of the TTA (time-displacement curve) of a suspension bridge was evaluated. Fig. 14 shows the adjusted seismic accelerations corresponding to the three different PGAs selected for this purpose. Subsequently, the reliability

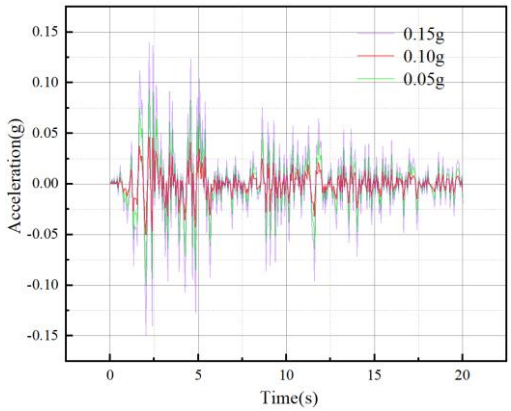

Fig. 14 Ground motion acceleration of three different PGA

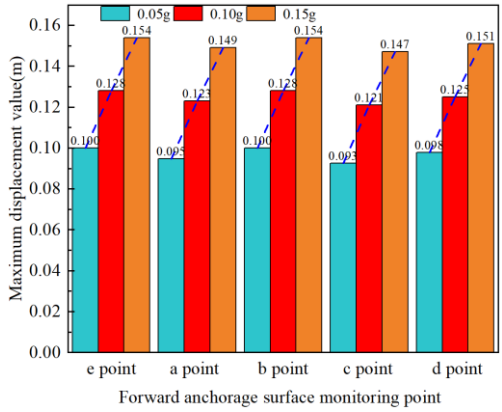

(a) The maximum displacement of different monitoring points on the front anchorage surface

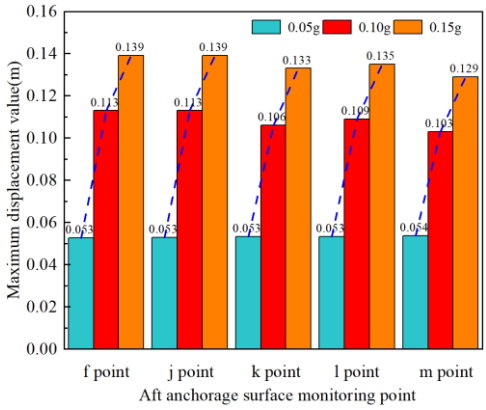

(b) The maximum displacement of different monitoring points on the back anchorage surface

Fig. 15 Displacement of different measuring points under three kinds of PGA

indices of the TTA at each measurement point were calculated according to Eqs. (6) to (7), as shown in Fig. 15.

As shown in Fig. 15, with increasing PGA values, the average maximum displacement of the front and rear anchor surfaces of the anchor plug also increases. When the PGA value is 0.05 g, the maximum displacement of the front anchor surface is reduced by 28.6% and 55.3% compared to when the PGA values are 0.1 g and 0.15 g, respectively. For the rear anchor face, the maximum displacement at a PGA value of 0.05 g is reduced by 109% and 155% compared to the values at PGA values of 0.1 g and 0.15 g, respectively. This indicates that the displacement responses of the front and rear anchor faces of the tunnel differ under different PGA values, with the rear anchor face being more sensitive to changes in PGA values. Under seismic excitation, the stress distribution and load transfer paths of the TTA structure cause the front and rear anchorage surfaces to experience different force conditions. Since the main cable force primarily acts on the rear anchorage surface during simulated normal operation of the TTA, the rear anchorage surface is more sensitive to changes in PGA values. The rear anchorage not only needs to transmit the inertial forces caused by seismic motion, but also needs to transmit the cable forces of the main cable. As the PGA value increases, the displacement response will be greater.

As can be seen from Fig. 16, the development of the plastic zone at the average point varies under different PGA values. With increasing PGA values, the plastic zone of the TTA surrounding rock continues to expand. At an earthquake acceleration of 0.05 g, the plastic zone is very small and almost non-existent, regardless of whether it is a tensile stress plastic zone or a shear stress plastic zone. However, when the PGA reached 0.1 g, the plastic zone of the TTA surrounding rock rapidly expanded, forming a tensile stress plastic zone around the TTA. This was mainly due to the enormous tensile stress exerted by the suspension bridge on the rear anchorage surface of the TTA, coupled with the effects of seismic acceleration, which made the “clamping effect” of the rock mass surrounding the TTA more pronounced.Under an earthquake acceleration of 0.15 g, the plastic zone further expanded, showing a more pronounced increase compared to 0.1 g, indicating that the rock mass surrounding the TTA is highly sensitive to changes in PGA values under different PGA conditions. The development of the plastic zone aligns with the trend of reliability changes shown in Fig. 17 for the TTA.

As demonstrated in Fig. 17, an increase in PGA value from 0.05 g to 0.1 g and subsequently to 0.15 g results in a gradual decrease in the reliability of the front and rear anchor surfaces. The figure illustrates that at a PGA value of 0.1 g or 0.15 g, there is a notable decline in reliability when compared to 0.The reliability of the front anchor face

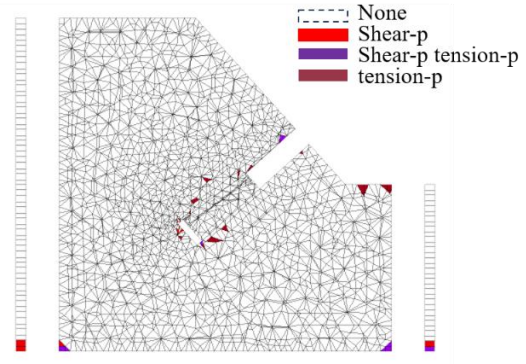

(a) Plastic zone distribution of TTA surrounding rock under 0.05 g ground motion acceleration

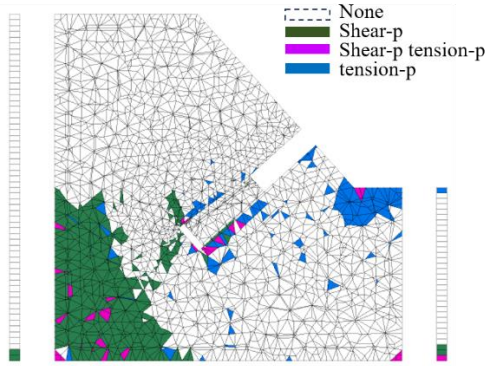

(b) Plastic zone distribution of TTA surrounding rock under 0.1 g ground motion acceleration

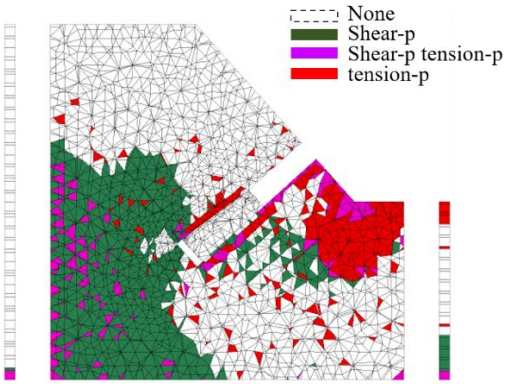

(c) Plastic zone distribution of TTA surrounding rock under 0.15 g ground motion acceleration

Fig.16 Plastic zone distribution of tunnel-type anchorage rock under different PGA

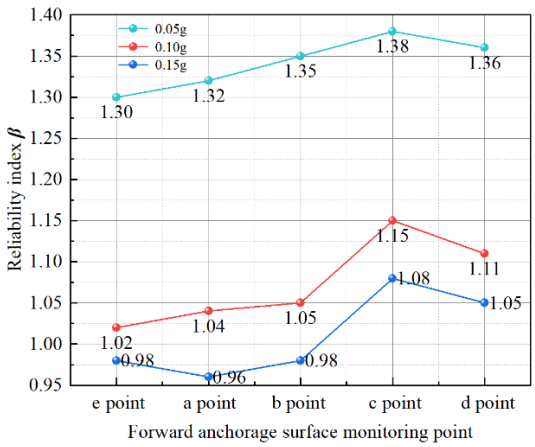

(a) Reliability of front anchorage surface under three different PGA

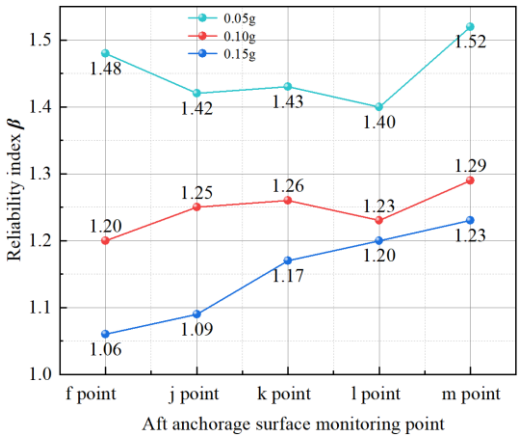

(b) Reliability of aft anchorage surface under three different PGA

Fig. 17 Reliability of front and rear anchorage surfaces under three different PGA

exhibits an average decrease of 25%, while the reliability of the rear anchor face demonstrates a decline of 16% and 26%, respectively. This phenomenon can be attributed to the observation that an increase in PGA values signifies an enhancement in earthquake intensity, consequently resulting in elevated impact forces on the TTA and its surrounding rock mass. It has been demonstrated that high-intensity seismic activity has a direct impact on the TTA, increasing the impact forces and stresses to which it is subjected. This, in turn, has a negative effect on the reliability of the TTA. This finding is consistent with the observed trend of the development of plastic zones within the TTA under different PGA values, indicating that the reliability of the TTA structure is highly sensitive to changes in PGA values. Conversely, as the PGA value increases, the reliability of TTA decreases accordingly, with a maximum decrease of up to 33%.

6. Conclusions

This study combined finite difference software and the second-order response surface method to model the TTA of Puli Bridge in Yunnan Province. Mathematical probability calculation methods were used to analyze rock parameters with high coefficients of variation. The dynamic response characteristics of the TTA structure under different working conditions were calculated, and specific rock parameters that significantly affect the dynamic response under seismic excitation were identified, as well as the differences in dynamic response between the front and rear anchorages. Having identified the root causes of these differences, we evaluated the reliability of TTA at different locations using data from numerical simulations, calculated the reliability under different PGA values, and analyzed the reasons for its decline. The specific conclusions are as follows:

- The TTA rock parameters obtained through mathematical probability and statistical calculations demonstrate that elastic modulus and cohesion significantly influence the dynamic response of TTA. Through the calculation of the coefficient of variation for various rock parameters in different TTA environments, it was determined that the coefficients of variation for elastic modulus and cohesion exceeded 0.2 in all surrounding rock parameters. This finding suggests that these parameters exert a more substantial influence on the dynamic response of TTA under seismic excitation.
- After calculating five operating conditions using finite difference software, the study found that the elastic modulus and cohesion of the surrounding rock in the TTA area have a significant impact on the dynamic response of the TTA. When the elastic modulus increases, the dynamic response of the TTA decreases; when the cohesion increases, the dynamic response increases. In addition, under seismic excitation, the dynamic response of the front anchor face is greater than that of the rear anchor face.
- Using the secondary sequence response surface method, it was calculated that the reliability of the front anchorage face of the suspension bridge TTA under seismic excitation is lower than that of the rear anchorage face, while the reliability of the lower part of the TTA is higher than that of the upper part. The weight of the anchor plug has a significant impact on the surrounding rock below, causing the rock to withstand greater compressive shear forces. This results in the dynamic response of the top of the TTA to ground movement being more intense than that of the bottom.
- By adjusting the size of the PGA, the reliability of TTA under three different PGA levels was calculated. The results showed that the reliability value of TTA is significantly affected by PGA. As PGA increases, the overall structural reliability of TTA gradually decreases, with a maximum decrease of 33%.

Subsequently, we will conduct scaling experiments and vibration table tests to more accurately simulate the dynamic response of TTA under seismic excitation. The objective of this study is to evaluate the reliability of TTA by combining probability and statistical methods. In addition, the study will provide reference and assistance for the reinforcement and design optimization of TTA prior to earthquakes.

Acknowledgments

The authors would like to acknowledge the financial support provided by “the National Natural Science Foundation of China (No.51808274,52168042)”, “China Postdoctoral Science Foundation (No.2019M653897XB)”, and Science and Technology Program of Gansu Province (No.22JR5RA250).

References

Ali, K., Saleem, A., Javed, A., Khadim, B. and Quadri, A.I. (2024), “A simplified approach for dynamic analysis of suspension bridges under extreme limit state”, *Pract. Period. Struct. Des. Constr.*, **29**(4). https://doi.org/10.1061/PPSCFX.SCENG-1523.

Anjneya, K. and Roy, K. (2021), “Response surface-based structural damage identification using dynamic responses”, *Structures*, **29**, 1047-1058. https://doi.org/10.1016/J.ISTRUC.2020.11.033.

Bossoto, B., Mboup, M. and Yger, A.A. (2023), “Structural stability of multidimensional systems: a test algorithm based on Monte-Carlo integration”, *Multidimens. Syst. Signal Pr.*, **34**(2), 479-502. https://doi.org/10.1007/S11045-023-00869-9.

Cao, Z. and Wang, X.X. (2015), “Stability reliability analysis of tailings dam based on quadratic polynomial sequential response surface method”, *China Min. Eng.*, **44**(1), 28-31.

Dederichs, A.C., Frøseth, G.T. and Øiseth, O. (2024), “Experimental comparison of three automatic operational modal analysis algorithms on suspension and floating bridges”, *Mech. Syst. Signal Pr.*, **215**, 111448-. https://doi.org/10.1016/J.YMSSP.2024.111448.

Dittmann, M., Schmidt, R. and Meyer, M. (2022), “Application of adjoint-enhanced first order second moment method for robust design optimization of a high pressure compressor rotor”, *J. Turbomach.*, 1-11. https://doi.org/10.1115/1.4055578.

Fernandez, C.D., Fenerci, A., Øiseth, O. and Wiig, P.Ø. (2022), “Investigations of the long-term extreme buffeting response of long-span bridges using importance sampling Monte Carlo simulations”, *Eng. Struct.*, 273. https://doi.org/10.1016/J.ENGSTRUCT.2022.114986.

Google, *Google Maps*, accessed June 6, 2025, https://http://www.gditu.net/

Han, Y.F., Liu, X.R., Du, L.B., Deng, Z.Y., Zhou, X.H., Xiao, Y., Zhang, G. and Lai, G.S. (2023), “Physical model test on the mechanical behavior and progressive failure of tunnel-type anchorages”, *Int. J. Rock Mech. Min. Sci.*, 169. https://doi.org/10.1016/J.IJRMMS.2023.105423.

Hu, J.C., Wang, X.C., Wang, Y.H., Huang, Y.X., Chai, T.S., Sun, K.J. and Wang, Z.N. (2024), “Analysis of dynamic characteristics of whipping effect on l-shaped main steam pipe considering fluid-structure interaction effect”, *Int. J. Impact Eng.*, **190**, 104988. https://doi.org/10.1016/J.IJIMPENG.2024.104988.

Huang, Q.X., Xu, X.T., Xu, C., Li, K. and Wang, J.L. (2016), “Dynamic response characteristics of an anchored rock slope during Wenchuan earthquake”, *Rock Soil Mech.*, **37**(6), 1729-1736. https://doi.org/10.16285/j.rsm.2016.06.025.

Joseph, O.A. (2024), “Determination of the geophysical signature

of soft-clay and hard lateritic soils and the implications on geotechnical works using electrical resistivity imaging", *Results Earth Sci.*, **2**, 100025-. https://doi.org/10.1016/J.RINES.2024.100025.

Khoshnevisan, S., Wang, L. and Juang, C.H. (2016), "Response surface-based robust geotechnical design of supported excavation – spreadsheet-based solution", *Georisk: Assessment and Management of Risk for Engineered Systems and Geohazards*, **11**(1), 90-102. https://doi.org/10.1080/17499518.2016.1247285.

Kranz, M., Lüdeker, J.K. and Kriegesmann, B. (2023), "A generalized approach for robust topology optimization using the first-order second-moment method for arbitrary response functions", *Struct. Multidiscip. O.*, **66**(5). https://doi.org/10.1007/S00158-023-03540-W.

Krüger, J.C., Kranz, M., Schmidt, T., Seifried, R. and Kriegesmann, B. (2023), "An efficient and non-intrusive approach for robust design optimization with the first-order second-moment method", *Comput. Method. Appl. M.*, 414. https://doi.org/10.1016/J.CMA.2023.116136.

Kumar, P.R, Muthukkumaran, K. and Sharma, C. (2024), "Technological advancements and sustainable practices in rock slope stability – Critical review", *Phys. Chem. Earth*, **136**, 103699-103699. https://doi.org/ 10.1016/J.PCE.2024.103699.

Li, X., Wei, H. and Wang, J.T. (2023), "Interval non-probabilistic reliability analysis of support structures for deep tunnels", *China Saf. Sci. J.*, **33**(12), 67-76.

Lim, H., Seo S., Ko, J. and Chung M. (2021), "Effect of joint characteristics and geometries on tunnel-type anchorage for suspension bridge", *Appl. Sci.*, **11**(24), 11688-11688. https://doi.org/10.3390/APP112411688.

Liu, X.R., Han, Y.F., Yu, C.T., Xiong, F., Zhou, X.H. and Deng, Z.Y. (2020), "Reliability assessment on stability of tunnel-type anchorages", *Comput. Geotech.*, 125. https://doi.org/10.1016/j.compgeo.2020.103661.

Małgorzata, B., Paweł, B. and Grzegorz, Ż. (2024), "Numerical analysis of a self-acting gas bearing lubricated with a low-boiling-point medium using an advanced model based on the finite difference methods and universal computational fluid dynamics software", *Appl. Sci.*, **14**(17), 7520-7520. https://doi.org/ 10.3390/APP14177520.

Namitha, R. and Vasugi K. (2024), "Synergistic effect of nano silica and metakaolin on mechanical and microstructural properties of concrete: An approach of response surface methodology", *Case Stud. Constr. Mater.*, **20**, e03196-. https://doi.org/10.1016/J.CSCM.2024.E03196,

Niccolò, B., Gianni, B. and Claudio, M.L. (2024), "Stability of suspension bridges in turbulent flow", *Nonlinear Dynam.*, **112**(19), 16711-16732. https://doi.org/10.1007/S11071-024-09931-Y.

Özge, A.K., Tuğba, E. and Ali, M. (2024), "Safety evaluation in the geotechnical site applications: A comprehensive analysis and forecasting model", *Saf. Sci.*, **173**, 106451. https://doi.org/10.1016/J.SSCI.2024.106451.

Paprocki, J., Stark, N., Lippman, T. and Graber, H.C. (2024), "Geotechnical investigation of exposed intertidal flats at the great bay estuary using sediment sampling and satellite-based synthetic aperture radar", *J. Waterw. Port, C.l Ocean Eng.*, **150**(4). https://doi.org/10.1061/JWPED5.WWENG-2051.

Rao, P.P., Wu, J., Jiang, G.Y., Shi, Y.W., Chen, Q.S. and Nimbalkar, S. (2021), "Seismic stability analysis for a two-stage slope", *Geomech. Eng.*, **27**(2), 189-196. https://doi.org/10.12989/gae.2021.27.2.189.

Sachin, J., Ulvi, R., Muhammad, A., Liang, C. and Subhamoy B. (2024), "Geotechnical challenges in monopile foundations and performance assessment of current design methodologies", *Ocean Eng.*, **310**(1), 118469-118469. https://doi.org/10.1016/J.OCEANENG.2024.118469.

Shen, Z.J., Jia, J.H., Jiang, N., Zhu, B. and Sun W.C. (2022), "Field-scale experiment on deformation characteristics and bearing capacity of tunnel-type anchorage of suspension bridge", *Energies*, **15**(13), 4772-4772. https://doi.org/10.3390/EN15134772.

Suzana, E., Ivan, D., Jurica, P., Marko, B. and Domagoj, D. (2024), "Determination of cable tension force in pedestrian suspension bridge short hangers based on finite element model updating", *J. Phys. Conference Series*, **2647**(12). https://doi.org/10.1088/1742-6596/2647/12/122013.

Taesuk, O., Inyup, K. and Yonghee, K. (2025), "Evaluation of effective kinetic parameters and adjoint flux distribution using iterated fission probability in the iMC Monte Carlo code", *Annal. Nuclear Energy*, **210**, 110878-110878. https://doi.org/10.1016/J.ANUCENE.2024.110878.

Taslimi, A. and Petrone, F. (2024), "Assessment of the seismic demands posed to suspension bridges in the near field with site-specific arrays of simulated ground motions", *J. Bridge Eng.*, **29**(5). https://doi.org/10.1061/JBENF2.BEENG-6353.

Usman, A., Sutanto, M.H., Napiah, M., Zoorob, S.E. and Al, S.A.M. (2021), "Optimization of irradiated waste polyethylene terephthalate modified asphalt pavement using response surface methodology", *Geomech. Eng.*, **26**(6), 513-527. https://doi.org/10.12989/gae.2021.26.6.513.

Van, Q.H., Trung, K.N. and Xuan, H.N. (2021), "Seismic analysis of soil-structure interaction: Experimentation and modeling", *Geomech. Eng.*, **27**(2), 115-121. https://doi.org/10.12989/gae.2021.27.2.115.

Verma, R.K., Singh, R., Kumar, V., Singh, T.N., Umrao, R.K., Mishra, P. and Sharma, P. (2024), "Statistical estimation of uniaxial compressive strength in geotechnical projects using regression analysis: a comparative study", *Int. J. Geomech.*, **24**(9). https://doi.org/10.1061/IJGNAI.GMENG-9384.

Wang, D.P., Wang, J.C., Sun, L.J., Niu, X. and Xu, Q. (2024), "Service reliability analysis of cracked lining under the influence of lining-surrounding rock age deterioration", *J. Railway Sci. Eng.*, **21**(6), 2535-2546.

Wang, D.Y., Tang, H., Yin, X.T., Yang, G.H. and Jiang, Y. (2020), "Estimation method of ultimate bearing capacity of tunnel-type anchorage based on simplified mechanical model", *Rock Soil Mech.*, **41**(10), 3405-3414.

Wu, A.Q., Zhang, Y.H., Luo, R., Xu, D.D., Fan, L., Zhou, H.M., Wu, X.C., Wu, Y.J. and Li, Y.J. (2023), "A field model test method of tunnel-type anchorages in rock mass and its application in railway suspension bridge engineering", *Rock Mech. Rock Eng.*, 56(12), 8891-8906. https://doi.org/10.1007/S00603-023-03534-6.

Yasir, I.S., Hu, Z.J. and Huang, J.W. (2024), "Main cable structure analysis and construction control of short span suspension bridge within three-tower", *Structures*, **69**, 107417-107417. https://doi.org/10.1016/J.ISTRUC.2024.107417.

Yu, C.T. (2021), "Stability and reliability study of tunnel-type anchorage", Master's Dissertation, *Chongqing University*, Chongqing, China.

GC